A Fluorescence Assay for Evaluating the Permeability of a Cardiac Microvascular Endothelial Barrier in a Rat Model of Ischemia/reperfusion
--Manuscript Draft--

Article Type:	Methods Article - JoVE Produced Video
Manuscript Number:	JoVE62746R2
Full Title:	A Fluorescence Assay for Evaluating the Permeability of a Cardiac Microvascular Endothelial Barrier in a Rat Model of Ischemia/reperfusion
Corresponding Author:	Yue-Jin Yang CHINA
Corresponding Author's Institution:	
Corresponding Author E-Mail:	yangyjfw@126.com
Order of Authors:	Yuejin Yang
	Ruijie Tang
	Kaihao Wang
	Yuyan Xiong
	Jian Meng
Additional Information:	
Question	**Response**
Please specify the section of the submitted manuscript.	Medicine
Please indicate whether this article will be Standard Access or Open Access.	Open Access ($3900)
Please indicate the **city, state/province, and country** where this article will be **filmed**. Please do not use abbreviations.	Beijing, China
Please confirm that you have read and agree to the terms and conditions of the author license agreement that applies below:	I agree to the Author License Agreement
Please provide any comments to the journal here.	See https://www.dropbox.com/request/JmEr19tUhVhtSNDrQKU5
Please confirm that you have read and agree to the terms and conditions of the video release that applies below:	I agree to the Video Release

1

TITLE:

A Fluorescence Assay for Evaluating the Permeability of a Cardiac Microvascular Endothelial Barrier in a Rat Model of Ischemia/reperfusion

AUTHORS AND AFFILIATIONS:

Ruijie Tang[1,*], Kaihao Wang[1,*], Yuyan Xiong[1], Jian Meng[2], Yuejin Yang[1]

[1]State Key Laboratory of Cardiovascular Disease, Department of Cardiology, Fuwai Hospital, National Center for Cardiovascular Diseases, Chinese Academy of Medical Sciences and Peking Union Medical College, Beijing, P. R. China
[2]State Key Laboratory of Cardiovascular Disease, Fuwai Hospital, National Center for Cardiovascular Diseases, Chinese Academy of Medical Sciences and Peking Union Medical College, Beijing, P. R. China
*These authors contributed equally to this study.

Email addresses of co-authors:

Ruijie Tang   (tangruijie1992@163.com)
Kaihao Wang   (1445347106@qq.com)
Yuyan Xiong   (xiongyuyan94@163.com)
Jian Meng   (mengjian2013@163.com)

Corresponding author:

Yuejin Yang   (yangyuejin_fw@126.com)

KEYWORDS:

Cardiac microvascular endothelial barrier, permeability, myocardial ischemia/reperfusion injury, FITC-dextran

SUMMARY:

Here, we describe a method to functionally assess the endothelial barrier of cardiac microvessels after ischemia/reperfusion injury via the measurement of the mean fluorescence intensity of extravasated 70,000 Da FITC-dextran in comparison with Evans Blue.

ABSTRACT:

Revascularization therapies for culprit arteries, regardless of percutaneous coronary intervention and coronary artery bypass grafting, are considered the best strategy for improving the clinical prognosis of patients with acute coronary syndrome (ACS). Nonetheless, myocardial reperfusion following effective revascularization can trigger significant cardiomyocyte death and coronary endothelial collapse, known as myocardial ischemia/reperfusion injury (MIRI). Usually, endothelial cells and their intercellular tight junctions cooperatively maintain the microvascular endothelial barrier and its relatively low permeability but fail in reperfusion areas.

45

46 Microvascular endothelial hyperpermeability induced by ischemia/reperfusion (IR)
47 contributes to myocardial edema, increased infiltration of pro-inflammatory cells, and
48 aggravated intramyocardial hemorrhage, which may worsen the prognosis of ACS. The
49 tracer used in this study—70,000 Da FITC-dextran, a branched glucose molecule
50 labeled by fluorescein isothiocyanate (FITC)—appears too large to infiltrate the cardiac
51 microvascular endothelium in normal conditions. However, it is capable of infiltrating
52 a broken barrier after MIRI. Thus, the higher the endothelial permeability is, the more
53 FITC-dextran accumulates in the extravascular intercellular space. Thus, the intensity
54 of fluorescence from FITC can indicate the permeability of the microvascular
55 endothelial barrier. This protocol takes advantage of FITC-dextran to evaluate the
56 cardiac microvascular endothelial barrier functionally, which is detected by an
57 automated quantitative pathology imaging system.

58

59 **INTRODUCTION:**
60 The fact that an increasing number of patients with coronary heart diseases have
61 benefited from revascularization therapies for decades does not negate the fatal
62 consequences of MIRI. As described by Yellon and Hausenloy, approximately 30% of
63 the final infarct size can be attributed to MIRI[1]. Cardiac microvascular endothelial
64 dysfunction is the core mechanism underlying MIRI and the "no-reflow" phenomenon
65 and is the target of many cardioprotective agents and classical cardioprotective
66 pathways[2]. Moreover, endothelial hyperpermeability of microvessels can trigger
67 myocardial edema[3] and the over-infiltration of pro-inflammatory cells, including
68 neutrophils[4], macrophages, and erthrocytes[5].

69

70 MIRI-induced oxidative stress and overexpressed pro-inflammatory cytokines, such as
71 the members of the tumor necrosis factor family[6] and the interleukin family[7], activate
72 signaling pathways of cell apoptosis to accelerate the death of ischemic myocardium.
73 Erythrocytes penetrate the vulnerable endothelial barrier and accumulate in the
74 extracellular matrix (ECM) to form intramyocardial hematoma[8]. Macrophage- and
75 neutrophil-derived matrix metalloproteinases disassemble collagen in the ECM, which
76 increases the risk of mechanical complication and post-infarction ventricular
77 aneurysm[9]. Thus, the permeability of the endothelial barrier is a crucial sign for the
78 prognostic evaluation of acute myocardial infarction and marks the severity of MIRI to
79 some degree.

80

81 FITC-dextran is an array of polysaccharides comprised of different lengths of branched
82 glucose molecules of molecular weight ranging from 4,000 Da to 70,000 Da. It is widely
83 used as the standard tracer to demonstrate the permeability of cell membranes,
84 functional physiological barriers such as the blood-brain barrier[10], and mucosal
85 membranes[11] under specific treatments and pathological conditions. The permeability
86 of one specific membrane varies for different substances according to their molecular
87 weights. Usually, albumin is restricted to cardiac microvessels; however, it can
88 penetrate the endothelium in the early stage of IR, causing myocardial edema. As the

89 molecular weight of albumin is approximately 68,000 Da, 70,000 Da FITC-dextran
90 would be a suitable agent to demonstrate endothelial hyperpermeability after IR.
91 Moreover, dextran has been widely adopted to maintain the blood volume and colloid
92 osmotic pressure of shock patients, and FITC-labeled tracers are used in numerous *in*
93 *vivo* or *in vitro* studies with few adverse effects.

94

95 In addition to FITC-dextran, endothelial permeability has been measured with Evans
96 Blue (EB) staining. After injection into the blood circulation, EB binds to serum albumin
97 tightly and forms a complex[12]. Thus, this EB–albumin complex, not EB alone, can be
98 used for the measurement of permeability, which means that the accuracy of such an
99 EB-based method can be influenced by different concentrations of serum albumin in
100 experimental subjects. Additionally, EB has been reported to poison the organs of
101 experimental animals, especially the heart, liver, and lungs, via cellular degeneration
102 and increased vascular permeability[13]. Endothelium undergoing ischemia/reperfusion
103 would be more sensitive to such detrimental effects than normal endothelium, which
104 can confound the significance of experimental results.

105

106 Compared to EB dye, FITC-dextran is exogenous, and the binding affinity to albumin is
107 negligible. Hence, FITC-dextran remains in the free state and is not bound by
108 macromolecules, such as albumin and tissue proteins. Thus, if administered according
109 to body weight, FITC-dextran can work at equal blood concentration and is not affected
110 by individual differences in serum albumin concentration and blood volume.
111 Tongxinluo (TXL), a traditional Chinese medicine, was used to test the diagnostic
112 sensitivity of this method. TXL reduces MIRI by maintaining the endothelial cellular
113 ultrastructure and endothelial barrier integrity[14]. TXL is also used to cure angina
114 pectoris and improve myocardial no-reflow after infarction clinically[15]. It contains
115 Radix ginseng, *Buthus martensi*, Hirudo, Eupolyphaga seu steleophaga, *Scolopendra*
116 *subspinipes*, Periostracum cicadae, Radix paeoniae rubra, Semen ziziphi spinosae,
117 Lignum dalbergiae odoriferae, Lignum santali albi, and Borneolum syntheticum. TXL
118 has been shown to protect the microvascular endothelium via the MEK/ERK pathway[16]
119 and endothelial nitric oxide synthase-mediated mechanisms[5,17] and alleviate
120 ischemia/reperfusion injury (IRI) of organs[18], especially the heart, in a dose-dependent
121 manner. Here, rats were fed with 0.5 g/kg TXL powder (an equivalent dose to that used
122 clinically in humans) as described[19]. This paper provides a method to functionally
123 assess the endothelial barrier of cardiac microvessels after IR via the measurement of
124 the total fluorescence intensity of extravasated 70,000 Da FITC-dextran compared to
125 EB.

126

127 **PROTOCOL:**

128

129 Animal experiments were performed in accordance with the "Guide for the Care and
130 Use of Laboratory Animals" issued by the US National Institutes of Health (Bethesda,
131 MD, USA, NIH Publication No. 85-23, revised 1996) and the "Regulation to the Care
132 and Use of Experimental Animals" of the Beijing Council on Animal Care (1996). The

133 study protocol was approved by the Care of Experimental Animals Committee of Fuwai
134 Hospital. Male SPF-class Sprague-Dawley rats (SD rats) weighing 150–180 g were used
135 in this study.
136
137 **1. Preparation of reagents, materials, and equipment**
138
139 1.1. Prepare reagents and solutions including 70% ethanol, FITC-dextran (70,000 Da,
140 dissolved in ice-cold saline to make 10% w/v solution for use), hair removal cream,
141 mounting medium with 4',6-diamidino-2-phenylindole (DAPI, 0.5–10 μg/mL), 1% w/v
142 EB/saline solution, and 5% w/v pentobarbital sodium/saline solution (stored in 4
143 °C in the dark).
144
145 1.2. Sterilize all surgical tools and materials in advance, including surgical tape; gauze
146 pads; surgical gloves; 16 G endotracheal tube; insulin syringe; operating scissors; large,
147 curved dissecting forceps; straight dissecting forceps; straight mosquito forceps;
148 curved mosquito forceps; retractors (30 mm Spread); 5 cm microneedle holders; 3-0
149 polypropylene suture (taper needle); and 6-0 polypropylene suture (round needle).
150
151 1.3. Check and ensure that all equipment, including the constant temperature
152 warming system, illumination system, ventilator, automated quantitative pathology
153 imaging system, and ultraviolet freezing slicer, are in good condition.
154
155 **2. Preparing the rats for the surgical procedures**
156
157 2.1. Divide all SD rats into Sham group, IR group, and TXL group (IR+TXL group)
158 randomly.
159
160 NOTE: In this protocol, six rats were randomly assigned to each group, n=6.
161
162 2.2. Weigh each SD rat, record the weight, and calculate the dose of TXL to be
163 administered for each rat.
164
165 2.3. Administer ibuprofen at a dose of 30 mg/kg by gavage to each rat at least 12
166 h prior to thoracotomy to alleviate preoperative pain and distress.
167
168 2.4. Administer a superfine powder of TXL at a dose of 0.5 g/kg by gavage 12 h
169 and 1 h to each SD rat in the IR+TXL group before anesthetization, as described[19].
170
171 2.5. Disinfect the operating table with 70% ethanol and place the sterilized
172 surgical tools and materials on the disinfected surface.
173
174 2.6. Adjust the temperature of the constant temperature warming system to
175 maintain the body temperature of the rats at 37 ± 1 °C.
176

3. Establish a rat model of cardiac ischemia/reperfusion

3.1. Inject 5% w/v pentobarbital sodium/phosphate-buffered saline (PBS) solution at a dose of 50 mg/kg (0.1 mL/100 g body weight) into the abdominal cavity to anesthetize the rat. Prepare the surgical site by carefully removing the fur from the neck to the chest by shaving or using a depilatory cream.

3.2. Gently adjust the position of the tongue as needed with sterilized tweezers and wipe respiratory secretion with sterilized cotton balls. Keep the glottis clearly in view and insert an endotracheal tube into the trachea gently.

3.3. Connect the endotracheal tube to a ventilator circling at 65–80 breaths per minute and adjust the tidal volume at 4–5 mL by fixing the rat's head and limbs.

3.4. Place a sterile drape over the rat, disinfect the operating area with tincture of iodine followed by 70% ethanol, and repeat this procedure three times.

3.5. Make a left parasternal incision at the level of the fourth intercostal space to expose the left musculus pectoralis major and pectoralis minor.

3.6. Dissect the fascia between the musculus pectoralis major and pectoralis minor using a blunt dissection technique to expose the left fourth intercostal space.

NOTE: Avoid excessive tissue damage and vascular injury that will cause severe bleeding and postoperative death.

3.7. Dissect the intercostal muscles, position a chest retractor within the fourth intercostal space, and then spread the ribs.

3.8. Tear the pericardium and remove the attached adipose tissue.

NOTE: Avoid damaging other organs with sharp surgical instruments, especially the lungs. Damage to the lungs can result in the development of pneumothorax and hemopneumothorax during the operation, causing cacoethic consequences ranging from hemodynamic disorders to reduced animal survival.

3.9. Manipulate the position of the thymus and expose the ascending aorta and left atria gently. Identify and ligate the proximal left anterior descending (LAD) artery transiently for 45 min with a 6-0 polypropylene suture (see **Figure 1 A-D**).

NOTE: This procedure is identical for sham control rats except that the LAD is not ligated.

3.10.   Remove the chest retractor and draw the ribs together in an interrupted

221 suture pattern with a 3-0 polypropylene suture.

222

223 3.11.   Restore negative intrathoracic pressure to ensure effective breathing.

224

225 NOTE: Two methods can be used to restore negative intrathoracic pressure: i)
226 before closing the chest cavity, researchers can plug up the air outlet of the
227 ventilator for 2 cycles to inflate the lungs. ii) The air remaining in the chest cavity
228 can be drawn out with a syringe after the intercostal space has been closed.

229

230 3.12.   After hair removal and disinfection, make an incision in the right lower
231 limb and dissect the superficial fascia from the right femoral vein.

232

233 3.13.   Loosen the ligation and check the respiration and circulation conditions
234 after inducing myocardial ischemia for 45 min.

235

236 3.14.   Inject 10% (w/v) FITC-dextran/saline solution into the femoral vein at 0.15
237 mL/100 g body weight, and press the femoral vein for 1 min with sterile cotton
238 balls to stanch the bleeding (**Figure 2A,B**).

239

240 NOTE: Alternatively, inject 1% w/v EB/saline solution into the femoral vein at a
241 dose of 0.5 mL/100 g body weight.

242

243 3.15.   Sew up the incisions with a 3-0 polypropylene suture and disinfect the
244 incisions, followed by postoperative analgesia with ibuprofen, as described above.

245

246 **4.   Preparation of frozen tissue slices for fluorescence measurement**

247

248 4.1. Inject 5% w/v pentobarbital sodium/PBS solution at a dose of 150 mg/kg (0.3
249 mL/100 g body weight) intraperitoneally to anesthetize the rats deeply after 3 h of
250 myocardial reperfusion.

251

252 4.2. Slit the abdominal cavity and expose the aorta abdominalis and vena cava (see
253 in **Figure 3A**).

254

255 4.3. Inject 50 mL of ice-cold PBS into the vena cava steadily, cut the aorta
256 abdominalis to flush blood from the myocardium, and harvest the heart.

257

258 NOTE: Observe changes in the lungs and liver. A sweating liver suggests that saline
259 is accurately injected into the vena cava (see in **Figure 3C**), and a pale lung is
260 considered a sign of a well-perfused myocardium (see in **Figure 3B**).

261

262 4.4. In a dark room, rinse the heart in ice-cold saline or PBS gently to remove any
263 remaining blood and FITC-dextran (or EB) from the chambers of the heart.

264

265 4.5. Cut off the heart from the ligation and discard the myocardium above the
266 ligation.
267
268 4.6. Embed the heart in molds with embedding compound followed by storage at
269 -80 °C.
270
271 4.7. Unload the frozen tissues from the embedding molds and load them on
272 sample holders in a prechilled -20 °C chamber of a freezing slicer.
273
274 4.8. Adjust the thickness of a single slice to 5–8 µm and slice the tissue at
275 approximately the midpoint of the base-apex axis (e.g., the middle of the
276 ischemia).
277
278 4.9. Load the sliced tissue on adhesive microscope slides and seal each slice with
279 one drop (approximately 40 µL) of fluorescent mounting medium containing DAPI.
280
281 4.10.   Keep the slides in a dry and dark box.
282
283 NOTE: If the slides cannot be scanned immediately, store them in a dry, cool, and
284 dark place to prevent the formation of condensate water and fluorescence
285 quenching.
286
287 **5.   Fluorescence measurement and data analysis**
288
289 5.1. Set up the imaging system and check the software connected to the scanner.
290
291 5.2. Load the slides in the slide shelves and insert them into the scanner.
292
293 5.3. Open the slide scanner software (see the **Table of Materials**) and set up a new
294 exposure protocol by clicking on **Edit Protocol | New….**
295
296 NOTE: If the scanner or its affiliated software is not available, a laser confocal
297 microscope (see the **Table of Materials**) or other ordinary slide scanners with the
298 fluorescence mode (see the **Table of Materials**) may be an alternative to the
299 automated quantitative fluorescence scanner.
300
301 5.4. Rename the protocol and study, and select the **fluorescence** mode.
302
303 5.5. Define **Whole Slide Scan | Pixel Resolution** and **Multispectral Regions | Pixel
304 Resolution** as **0.25 µm (40x)** respectively.
305
306 5.6. Click on **Edit Filters and Bands…** to select the **Whole Slide Scan Filters** column
307 and the **Multispectral Region Bands** column.
308

309 NOTE: If EB is used, select **Whole Slide Scan Filters | DAPI** and **Texas Red or AF495**.
310 If FITC-dextran is used, select **Multispectral Region Bands | DAPI** and **FITC or**
311 **AF488**.

312

313 5.7. Click on **Edit Exposures...** and load the carrier.

314

315 5.8. Select the target slot and click on **Take overview**.

316

317 NOTE: This takes a brightfield scan of each heart section. Select the myocardium
318 for focusing or select the area blindly.

319

320 5.9. Select the target slide, adjust **Stage Height** to approximately -50 μm, and click
321 on **Auto Focus**.

322

323 5.10.   Click on **Whole Scan Exposure(ms)-DAPI | Autoexpose**.

324

325 NOTE: The exposure time of DAPI for each slide does not have to be the same
326 because images with DAPI are used to illustrate cross-sections of the heart, which
327 are convenient for outlining the area of the myocardium but not to calculate
328 fluorescence density.

329

330 5.11.   Click on **Whole Scan Exposure(ms)-FITC | Autoexpose**.

331

332 NOTE: Click on **Whole Scan Exposure(ms)-Texas Red | Autoexpose** if using EB. It
333 is important to remember and ensure that the exposure time of FITC or Texas Red
334 is the same in all slide scans.

335

336 5.12.   Click on **Auto Focus** again and ensure that the slide is in focus.

337

338 5.13.   Click on **Back** and save the protocol.

339

340 5.14.   Repeat steps 5.7–5.14 for each slide.

341

342 5.15.   Return to the home page and click on **Scan Slides**.

343

344 5.16.   Select a slot, rename all the slides, and select the corresponding exposure
345 protocol for each slide.

346

347 5.17.   Scan the slides and capture the images.

348

349 5.18.   Open the images with slide viewer software for the scans (see the **Table**
350 **of Materials**).

351

352 5.19.   Magnify all the images to a relatively equal extent.

353

5.20.   Snapshot and save images as .tiff.

NOTE: It is better to save the images with and without scale bars at the same time. Images with scale bars can be used for publication, whereas those without scale bars can be used for statistical analysis.

5.21.   Open ImageJ software, click on **Analyze**, and select **Set Measurement**.

5.22.   Select **Area | Integrated density**.

5.23.   Open the image in the FITC channel with Image J.

5.24.   Click on **Analyze** again and record the numerical value of integrated density (**IntDen**) that appears.

NOTE: As scale bars in the images can be mistaken for grayscale of fluorescence by computers, use images without scale bars to measure IntDen.

5.25.   Close the FITC image and open the image in the DAPI channel.

5.26.   Outline a cross-section of the myocardium.

5.27.   Click on **Analyze** and collect **Area** data.

5.28.   Calculate the ratios of IntDen/Area (mean of fluorescence) for each heart.

5.29.   Input all ratios in statistical analysis software.

REPRESENTATIVE RESULTS:
Before performing the FITC-dextran assay to evaluate the changes in cardiac endothelial permeability after IR, we strongly recommend that experiments be conducted by the same researcher specializing in the establishment of myocardial IR model in rats to confirm that the coronary arteries are occluded in the same position successfully, and the ratios of ischemic area/total area are constant among all rats. As shown in **Figure 1A,B**, the heart (indicated by yellow arrow) was exposed, and a loop (indicated by green arrow) was formed in the myocardium located in the anterior wall of the left ventricle, approximately 2 mm under the edge of the left atrial appendage with a 0.5 mm (inner diameter) capillary silicone tube and 6-0 suture. As seen in **Figure 1C**, when the loop was fastened, the ischemic myocardium turned from pink to greyish pink (indicated by the white arrow) immediately.

Moreover, the myocardium reperfused and recovered its pink color immediately

after the loop was loosened, as illustrated in **Figure 1D**. After loosening the loop, an incision was made parallel to the long axis of the femur in the inner thigh. The femoral vein was exposed and punctured with an insulin syringe, as shown in **Figure 2A,B**. Following a 3 h reperfusion, a "V" incision was made in the lower abdomen, and the aorta abdominalis and vena cava were dissected from the peritoneum (**Figure 3A**). Cold saline was injected into the vena cava gently, and the aorta abdominalis was cut to prevent the ventricular wall from being stretched excessively due to the intraventricular pressure that would affect its histopathological structure. Bleached lungs (red arrow in **Figure 3B**) and liver in **Figure 3C** indicate that the tissue was well-reperfused with saline.

Consequently, there was no significant difference in the cross-sectional area among the three groups: 1.00 ± 0.08 in the Sham group vs. 0.97 ± 0.08 in the IR group vs. 1.02 ± 0.04 in the IR+TXL group (**Figure 4A**, n = 6 in each group, p > 0.05 between any two groups). As shown in **Figure 4B,C**, the mean intensity of green fluorescence in the whole sections from Sham rats was extremely low. In contrast, fluorescence emitted by extravasated FITC-dextran increased markedly in the IR group, normalized to the Sham group (5.52 ± 0.85 in the IR group vs. 1.00 ± 0.19 in the Sham group, n = 6, p < 0.05). Furthermore, TXL superfine powder, known to protect the cardiac microvascular endothelium[14,16], remarkably reversed the higher fluorescence intensity induced by IR (2.87 ± 0.52 in IR+TXL group vs. 5.52 ± 0.85 in IR group, n = 6, p < 0.05). The images of the regional myocardium indicated that FITC-dextran overwhelmingly accumulated in the extracellular matrix but not in the microvessels, and that TXL improved endothelial barrier function (**Figure 5**).

Compared with FITC-dextran, EB may be a suboptimal alternative because EB is inferior to 70,000 Da FITC-dextran in both image quality and sensitivity. Similarly, there was no significant difference in the cross-sectional area among the three groups: 1.00 ± 0.08 in the Sham group vs. 0.97 ± 0.08 in the IR group vs. 0.98 ± 0.05 in the IR+TXL group (**Supplemental Figure S1A**, n = 6 in each group, p > 0.05 between any two groups). As shown in **Supplemental Figure S1B,C**, the mean intensity of red fluorescence in whole cross-sections from Sham rats was relatively higher, especially in the endocardium and epicardium. Although red fluorescence emitted by EB increased sharply in the IR group (4.41 ± 0.66 in the IR group vs. 1.00 ± 0.22 in the Sham group, n = 6, p < 0.05), the difference between the IR+TXL and IR groups was not significant (3.73 ± 0.47 in the IR+TXL group vs. 4.41 ± 0.66 in the IR group, n = 6, p = 0.0956).

Furthermore, this method was tested in a myocardial infarction (MI) model (**Supplemental Figure S2**). In the **M**yocardial **I**nfarction **I**njection first (MII) group, FITC-dextran solution (at the same concentration mentioned earlier) was injected into the circulation 5 min before LAD ligation. This was in contrast to the FITC-dextran solution injected immediately after ligation in the MIL rats (**M**yocardial **I**nfarction **L**igation first) described earlier in this protocol. Interestingly, only low

441 amounts of FITC-dextran extravasated into the ECM of the injured myocardium in
442 MI rats of both groups, indicated by weak green fluorescence intensity in
443 **Supplemental Figure S2**.

444

445 **FIGURE AND TABLE LEGENDS:**
446 **Figure 1: Visual field of thoracotomy and establishment of ischemia/reperfusion in a**
447 **rat model.** (**A**) Exposing the rat's heart (indicated by yellow arrow); (**B**) forming a loop
448 to encircle the coronary artery (indicated by green arrow); (**C**) fastening the loop and
449 inducing myocardial ischemia for 45 min (indicated by white arrow); (**D**) loosening the
450 loop and allowing myocardial reperfusion for 3 h (indicated by the blue arrow).

451

452 **Figure 2: Dissection of the femoral vein and intravenous injection.** (**A**) Exposing the
453 femoral vein (the femoral nerve is indicated by the arrow on the left; the femoral artery
454 is indicated by the arrow in the middle; the femoral vein is indicated by the arrow on
455 the right). (**B**) Injecting FITC-dextran solution into the femoral vein with an insulin
456 syringe. Abbreviation: FITC = fluorescein isothiocyanate.

457

458 **Figure 3: Tissue perfusion and symptoms of efficient perfusion.** (**A**) Dissecting the
459 abdominal aorta and the vena cava (the abdominal aorta is indicated by the white
460 arrow; the vena cava is indicated by the black arrow). (**B**) Bleached lungs are a
461 symptom of adequate perfusion; (**C**) bleached mucosa, bleached kidney, and sweating
462 liver are all symptoms of adequate perfusion (red arrow: mucosa; white arrow: liver;
463 black arrow: kidney).

464

465 **Figure 4: Representative images and analysis of mean fluorescence intensity by FITC-**
466 **dextran staining.** (**A**) Relative cross-sectional area of each group normalized to that of
467 the Sham group ($p > 0.05$); (**B**) relative fluorescence intensity in the FITC channel of
468 each group normalized to that of the Sham group; (**C**) representative images at 9.5x
469 magnification in each group. Scale bars = 800 μm. One-way ANOVA with Tukey's *post-*
470 *hoc* multiple-group comparisons. * vs. Sham group, $p < 0.05$; # vs. IR group, $p < 0.05$.
471 Bar graphs show group mean ± SD. Abbreviations: IR = ischemia/reperfusion; TXL =
472 Tongxinluo; FITC = fluorescein isothiocyanate; DAPI = 4',6-diamidino-2-phenylindole;
473 ANOVA = analysis of variance; SD = standard deviation.

474

475 **Figure 5: Representative images of areas of interest at 200x magnification of each**
476 **group after FITC-dextran staining.** Scale bars = 50 μm. Abbreviations: FITC =
477 fluorescein isothiocyanate; DAPI = 4',6-diamidino-2-phenylindole.

478

479 **Supplemental Figure S1: Representative images and analysis of mean fluorescence**
480 **intensity by Evans Blue staining.** (**A**) Relative cross-sectional area of each group
481 normalized to that of the Sham group ($p > 0.05$); (**B**) relative fluorescence intensity in
482 the Texas red channel of each group normalized to that of the Sham group; (**C**)
483 representative images in each group. One-way ANOVA with Tukey's *post-hoc* multiple-
484 group comparisons. Scale bars = 800 μm. * vs. Sham group, $p < 0.05$. Bar graphs show

485 group mean ± SD. Abbreviations: IR = ischemia/reperfusion; TXL = Tongxinluo; DAPI
486 = 4',6-diamidino-2-phenylindole; ANOVA = analysis of variance; SD = standard
487 deviation.
488
489 **Supplemental Figure S2: Representative images at 9.5x magnification of FITC-dextran**
490 **staining in a myocardial infarction model.** Scale bars = 800 µm. Abbreviations: MII =
491 myocardial infarction injection first (inject FITC-dextran before myocardial infarction);
492 MIL = myocardial infarction ligation first (inject FITC-dextran immediately after
493 myocardial infarction); FITC = fluorescein isothiocyanate; DAPI = 4',6-diamidino-2-
494 phenylindole.
495
496 **DISCUSSION:**
497 This paper presents a protocol to assess the dysfunction of the cardiac endothelial
498 barrier after being exposed to MIRI. It should be noted that there are several
499 crucial steps in this protocol that determine the reliability and accuracy of the
500 results. All steps involving FITC-dextran are to be performed in a dark room. The
501 FITC-dextran/saline solutions must be stored at 4 °C and wrapped with tin foil.
502 Additionally, coronary arteries must be ligated, as illustrated in **Figure 1**, so that
503 the myocardium can be reperfused immediately after the loop is loosened.
504 Researchers can choose 5-0 or 6-0 polyethylene sutures because thinner strings
505 under 7-0 are more likely to cut myocardial fibers and vessels. Importantly, the
506 tracer solution should be injected into the femoral veins and not the tail veins.
507 Each heart should be well-perfused and well-rinsed with ice-cold saline before and
508 after being sacrificed, respectively.
509
510 Many researchers specializing in MIRI are inclined to study the disrupted
511 subcellular structure of the endothelium in the earlier stage of myocardial
512 reperfusion—the formation of apoptotic bodies, swelling mitochondria, and
513 abnormal intercellular junctions—to prove the hyperpermeability of the
514 endothelium via electron microscopic examination. Immunoblotting has also been
515 used to measure microvascular permeability because the decrease in levels of
516 tight conjunction proteins is regarded as the core mechanism of endothelial injury
517 and malfunction of endothelial barrier over time. For instance, VE-cadherin[20] and
518 β-catenin[21] are key elements of endothelial cell-to-cell adhesion junctions, and
519 these connections contribute to the maintenance of vascular integrity[22]. Tight
520 junctions, such as JAM-A[23,24] and occludin[25], also cooperatively participate in the
521 construction of the endothelial barrier in the circulatory system.
522
523 Currently, an increasing number of studies suggest that mitochondrial function
524 and mitochondrial homeostasis could be key targets of protective pathways
525 against reperfusion injury. As reported in pathophysiological and pharmacological
526 studies, mitophagy can play an important role in the cellular death of the
527 endothelium and myocardium induced by IR[26]. In addition, mitochondrial fission,
528 mitochondrial proteostasis, and mitochondrial quality control may protect high-

529 risk myocardium in reperfused areas[27,28]. The above methods focus more on
530 demonstrating different mechanisms or causes of hyperpermeability than on
531 displaying endothelial permeability directly and visually. Moreover, sample
532 preparation for electron microscopic examination is complicated and dangerous.
533 Glutaraldehyde, acetone, and osmic acid solutions used in electron microscopy
534 probably volatilize and erode the mucosa, conjunctiva, and skin, even threatening
535 lives if used in uncontrolled environments.
536
537 Compared to these indirect and life-threatening methods, this method, which
538 measures the fluorescence intensity emitted by FITC-dextran extravasation, is
539 ideal for assessing cardiac microvascular permeability. First, 70,000 Da FITC-
540 dextran cannot penetrate through the endothelium under normal physiological
541 conditions but can enter the myocardial interstitial space under IR, which allows a
542 clear differentiation between rats under different treatments. Additionally, the
543 FITC-dextran solution is injected into the blood via the femoral veins, which
544 guarantees that all of the fluid is injected into the rat's circulation. In contrast, tail
545 vein injection is more difficult in rats because the tail vein is indistinct and covered
546 with a thick stratum. Further, unlike regular paraformaldehyde fixation and
547 paraffin embedding, myocardial tissue treatment is simplified and optimized using
548 the quick-freeze pathological section technique used in this study. Short storage
549 time, light-proof environment, and cryopreservation may together alleviate
550 fluorescence quenching of FITC.
551
552 More importantly, this method can minimize selection bias during statistical
553 analysis. We perform sufficient heart perfusion with saline to ensure that nearly
554 all the blood mixed with FITC-dextran is douched out from the myocardium and
555 the heart chambers, which can eliminate the fluorescence emitted by any FITC
556 remaining in the vessels. If this is not the case, fluorescence merged with
557 capillaries should be excluded and trimmed artificially. While collecting tissue
558 from areas of interest, no visual boundary was observed between the ischemic
559 myocardium and the remote myocardium, especially after EB dye staining. This
560 hindered the collection of samples from these representative areas. Using the
561 method described herein, researchers can obtain images of whole sections and
562 analyze the fluorescence intensity using a quantitative slider scanner.
563
564 Interestingly, EB dye can be an alternative, albeit suboptimal, to FITC-dextran.
565 Compared with the relatively harsh storage conditions of FITC-dextran, EB powder
566 or its solution can remain stable at room temperature for a long time. Additionally,
567 EB is relatively inexpensive for most institutions. Nonetheless, certain
568 disadvantages could limit its application. First, EB staining shows lower sensitivity
569 than FITC-dextran, which may underestimate the differences among groups and
570 increase the sample size of each group. Besides, EB shows stronger adhesion to
571 proteins. The endocardium and epicardium are more easily stained by EB, which
572 can influence the results of fluorescence density. Further, obvious filling defects in

573 the reperfusion area remarkedly reduce the image quality, which can limit the use
574 of EB.

576 To extend the application of this method in an MI model, the method was tested
577 in an MI model. First, FITC-dextran was injected into blood vessels after LAD
578 ligation. As expected, a low level of fluorescence was emitted from the slice
579 because FITC-dextran in blood flow cannot pass through the ligated site, and no
580 FITC-dextran entered the ischemic area. FITC-dextran was also applied 5 min
581 before ligation to ensure the passage of FITC-dextran into all organs. Consequently,
582 FITC-dextran failed to penetrate the microvascular endothelium probably because
583 no perfusion pressure in ligated blood vessels can drive FITC-dextran through the
584 endothelium. Generally, this method probably requires significantly more
585 modification to satisfy its application in the MI model.

587 Despite the above advantages, there are limitations to this method. First, this
588 protocol was not tested in IR models of other animals, which may limit its
589 application in preclinical and clinical studies. Second, FITC-labeled dyes are more
590 expensive than other common dyes such as EB. However, unlike EB, as 10% w/v
591 FITC-dextran solution, diluted with serum, rarely changes the color of the
592 myocardium, FITC-dextran staining and EB/2,3,5-triphenyltetrazole chloride (TTC)
593 dual staining may be conducted in the same heart, which can trim the budget with
594 respect to the number of animals and the dyes used. Last, the slide scanner used
595 in this study—the Quantitative Slide Scanner and similar instruments—may not be
596 available in some laboratories. In summary, this protocol presents a simplified,
597 reliable, and visual method for the detection of cardiac microvascular endothelial
598 permeability in an IR model in rats using a fluorescence assay based on an
599 automated quantitative pathology imaging system. This protocol demonstrates
600 that 70,000 Da FITC-dextran performs better than EB in the functional assessment
601 of the endothelial barrier of cardiac microvessels after IR injury.

608 **DISCLOSURES:**
609 The authors declare no conflicts of interest.

611 **REFERENCES:**
612 1.   Yellon, D. M., Hausenloy, D. J. Myocardial reperfusion injury. *New England Journal*
613 *of Medicine*. **357** (11), 1121–1135 (2007).
614 2.   Hausenloy, D. J. et al. The coronary circulation in acute myocardial
615 ischaemia/reperfusion injury: a target for cardioprotection. *Cardiovascular Research*.
616 **115** (7), 1143–1155 (2019).

617   3.   Tada, Y., Yang, P. C. Myocardial edema on T2-weighted MRI: new marker of
618   ischemia reperfusion injury and adverse myocardial remodeling. *Circulation Research*.
619   **121** (4), 326–328 (2017).

620   4.   Chandrasekar, B., Smith, J. B., Freeman, G. L. Ischemia-reperfusion of rat
621   myocardium activates nuclear factor-KappaB and induces neutrophil infiltration via
622   lipopolysaccharide-induced CXC chemokine. *Circulation*. **103** (18), 2296–2302 (2001).

623   5.   Li, X. -D. et al. Tongxinluo reduces myocardial no-reflow and ischemia-reperfusion
624   injury by stimulating the phosphorylation of eNOS via the PKA pathway. *American
625   Journal of Physiology. Heart and Circulatory Physiology*. **299** (4), H1255-61 (2010).

626   6.   Pei, H. et al. TNF-α inhibitor protects against myocardial ischemia/reperfusion
627   injury via Notch1-mediated suppression of oxidative/nitrative stress. *Free Radical
628   Biology & Medicine*. **82**, 114–121 (2015).

629   7.   Liao, Y. -H. et al. Interleukin-17A contributes to myocardial ischemia/reperfusion
630   injury by regulating cardiomyocyte apoptosis and neutrophil infiltration. *Journal of the
631   American College of Cardiology*. **59** (4), 420–429 (2012).

632   8.   Pedersen, S. F. et al. Assessment of intramyocardial hemorrhage by T1-weighted
633   cardiovascular magnetic resonance in reperfused acute myocardial infarction. *Journal
634   of Cardiovascular Magnetic Resonance*. **14** (1), 59 (2012).

635   9.   Fang, L. et al. Differences in inflammation, MMP activation and collagen damage
636   account for gender difference in murine cardiac rupture following myocardial
637   infarction. *Journal of Molecular and Cellular Cardiology*. **43** (5), 535–544 (2007).

638   10. Xu, Y. et al. Quantifying blood-brain-barrier leakage using a combination of evans
639   blue and high molecular weight FITC-Dextran. *Journal of Neuroscience Methods*. **325**,
640   108349 (2019).

641   11. Li, B. -R. et al. In vitro and in vivo approaches to determine intestinal epithelial cell
642   permeability. *Journal of Visualized Experiments: JoVE*. **140**, 57032 (2018).

643   12. Yao, L., Xue, X., Yu, P., Ni, Y., Chen, F. Evans Blue dye: a revisit of its applications in
644   biomedicine. *Contrast Media & Molecular Imaging*. **2018**, 7628037 (2018).

645   13. Roberts, L. N. Evans blue toxicity. *Canadian Medical Association Journal*. **71** (5),
646   489–491 (1954).

647   14. Qi, K. et al. Tongxinluo attenuates reperfusion injury in diabetic hearts by
648   angiopoietin-like 4-mediated protection of endothelial barrier integrity via PPAR-α
649   pathway. *PLoS One*. **13** (6), e0198403 (2018).

650   15. Zhang, H. -T. et al. No-reflow protection and long-term efficacy for acute
651   myocardial infarction with Tongxinluo: a randomized double-blind placebo-controlled
652   multicenter clinical trial (ENLEAT Trial). *Chinese Medical Journal (English)*. **123** (20),
653   2858–2864 (2010).

654   16. Cui, H. et al. Induction of autophagy by Tongxinluo through the MEK/ERK pathway
655   protects human cardiac microvascular endothelial cells from hypoxia/reoxygenation
656   injury. *Journal of Cardiovascular Pharmacology*. **64** (2), 180–190 (2014).

657   17. Chen, G. -H. et al. Inhibition of miR-128-3p by Tongxinluo protects human
658   cardiomyocytes from ischemia/reperfusion injury via upregulation of p70s6k1/p-
659   p70s6k1. *Frontiers in Pharmacology*. **8**, 775 (2017).

660   18. Yu, Z. -H. et al. PI3K/Akt pathway contributes to neuroprotective effect of

Tongxinluo against focal cerebral ischemia and reperfusion injury in rats. *Journal of Ethnopharmacology*. **181**, 8–19 (2016).

19. Yang, H. -X., Wang, P., Wang, N. -N., Li, S. -D., Yang, M. -H. Tongxinluo ameliorates myocardial ischemia-reperfusion injury mainly via activating Parkin-mediated mitophagy and downregulating ubiquitin-proteasome system. *Chinese Journal of Integrative Medicine*. doi: 10.1007/s11655-019-3166-8 (2019).

20. Pulous, F. E., Grimsley-Myers, C. M., Kansal, S., Kowalczyk, A. P., Petrich, B. G. Talin-dependent integrin activation regulates VE-cadherin localization and endothelial cell barrier function. *Circulation Research*. **124** (6), 891–903 (2019).

21. Cong, X., Kong, W. Endothelial tight junctions and their regulatory signaling pathways in vascular homeostasis and disease. *Cellular Signaling*. **66**, 109485 (2020).

22. Giannotta, M., Trani, M., Dejana, E. VE-cadherin and endothelial adherens junctions: active guardians of vascular integrity. *Developmental Cell*. **26** (5), 441–454 (2013).

23. Monteiro, A. C., Parkos, C. A. Intracellular mediators of JAM-A-dependent epithelial barrier function. *Annals of the New York Academy of Sciences*. **1257**, 115–124 (2012).

24. Kakogiannos, N. et al. JAM-A acts via C/EBP-α to promote Claudin-5 expression and enhance endothelial barrier function. *Circulation Research*. **127** (8), 1056–1073 (2020).

25. Feldman, G. J., Mullin, J. M., Ryan, M. P. Occludin: structure, function and regulation. *Advanced Drug Delivery Reviews*. **57** (6), 883–917 (2005).

26. Zhou, H. et al. NR4A1 aggravates the cardiac microvascular ischemia reperfusion injury through suppressing FUNDC1-mediated mitophagy and promoting Mff-required mitochondrial fission by CK2α. *Basic Research in Cardiology*. **113** (4), 23 (2018).

27. Wang, J., Toan, S., Zhou, H. Mitochondrial quality control in cardiac microvascular ischemia-reperfusion injury: New insights into the mechanisms and therapeutic potentials. *Pharmacological Research*. **156**, 104771 (2020).

28. Zhu, H. et al. Phosphoglycerate mutase 5 exacerbates cardiac ischemia-reperfusion injury through disrupting mitochondrial quality control. *Redox Biology*. **38**, 101777 (2021).

Figure 1   Click here to access/download;Figure;Figure 1 (2).tif ⬇
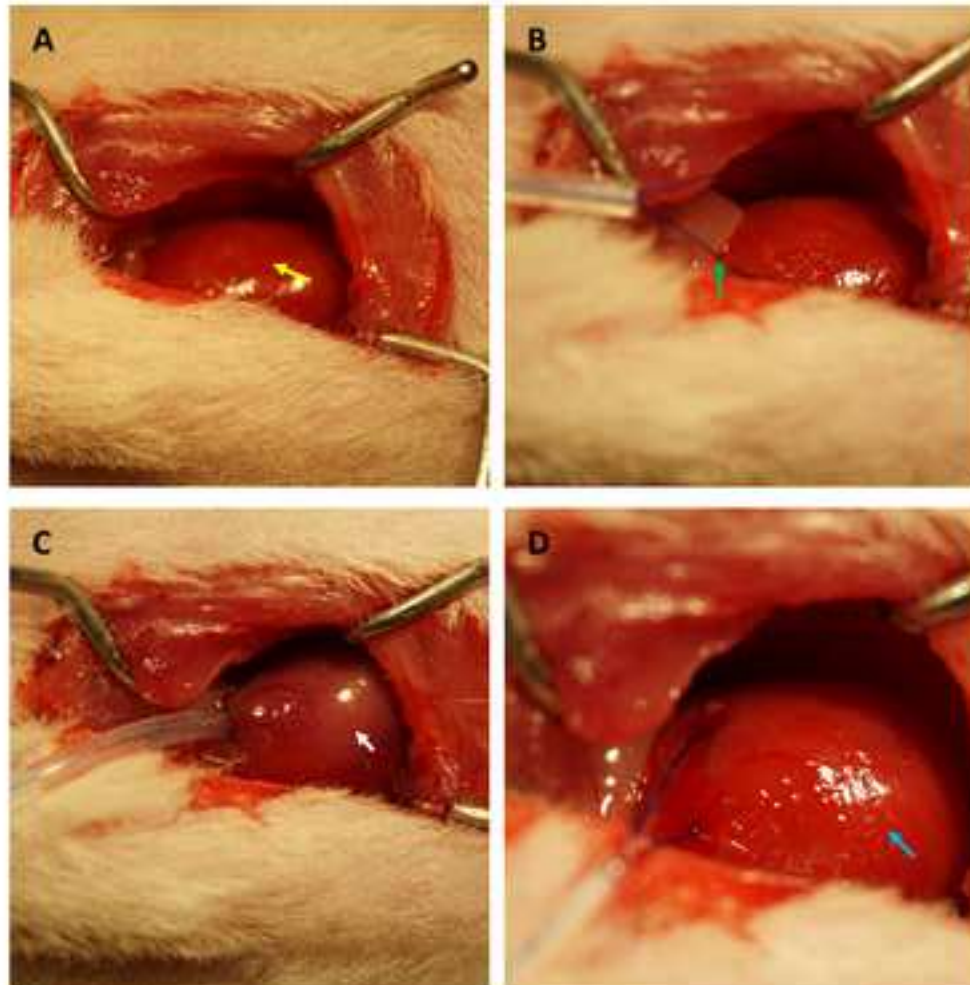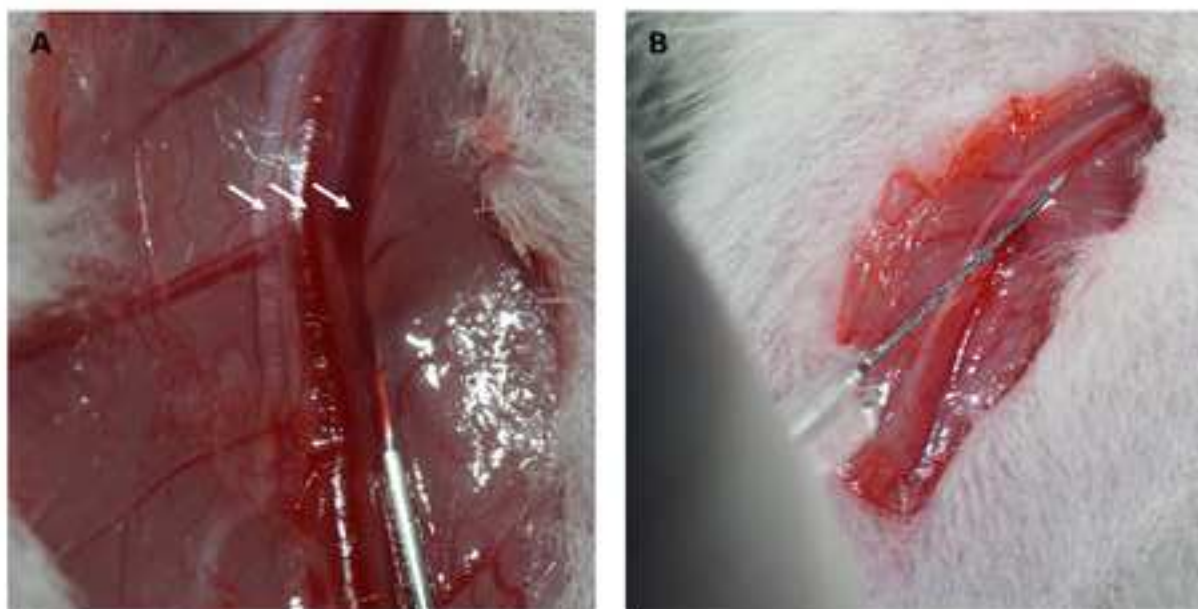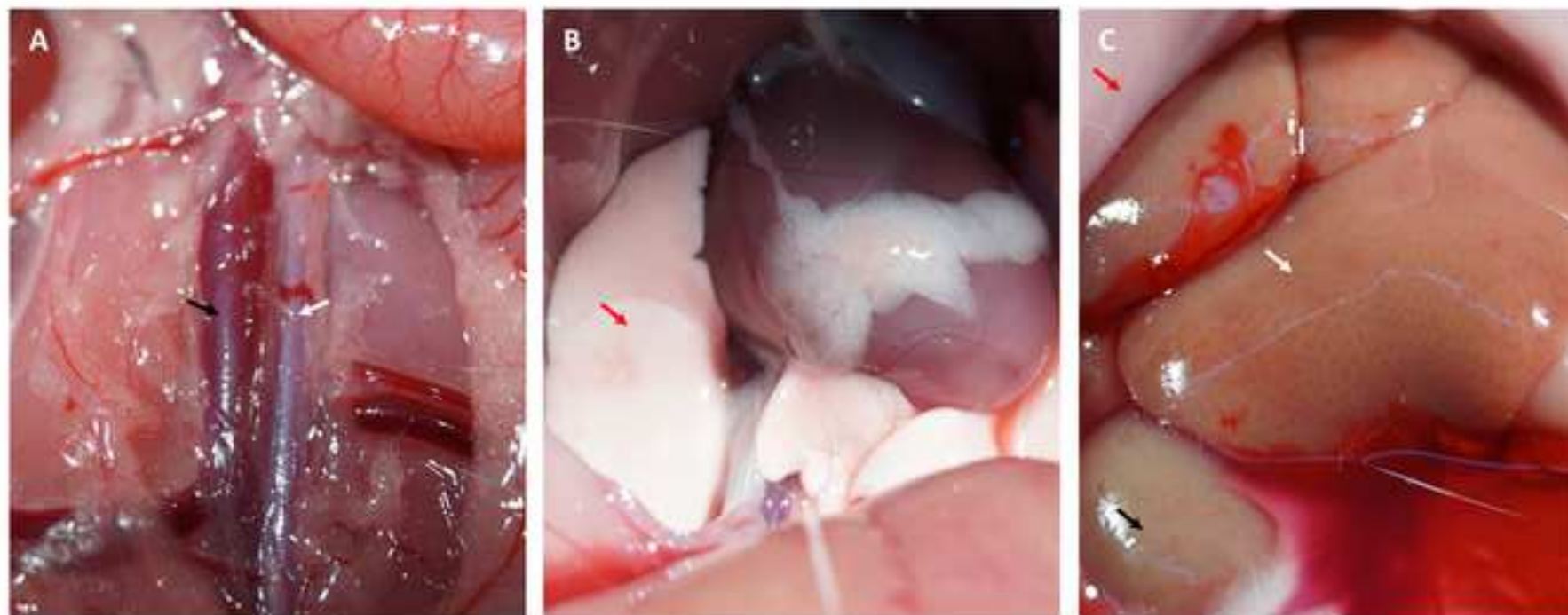
Click here to access/download
Table of Materials
JoVE_Materials 6.9.xls

Dear Editors:

Thank you for comments and suggestions. We have tried our best to made any proper changes according to Editorial comments and answer questions from Reviewers.

ANSWERS TO Reviewer 1

We are very grateful for your opinions and suggestions.

Comment 1 The author needs to standardize the citation of references. Where is the first reference cited in the text? Why is the journal name of the second reference not included?

For Comment 1

All citations have been modified.

Comment 2 What is the basis for the dosage of Tongxinluo? The corresponding references are needed.

For Comment 2

According to published articles, Tongxinluo are usually used at the dose of 0.4g/kg-0.5g/kg in rats, so we decided feed rats with TXL at the dose of 0.5g/kg and have cited corresponding references in our new manuscript.

[**Reference**: Yang HX, Wang P, Yang MH. Tongxinluo Ameliorates Myocardial Ischemia-Reperfusion Injury Mainly via Activating Parkin-Mediated Mitophagy and Downregulating Ubiquitin-Proteasome System. Chin J Integr Med. 2019 Jun 21. doi: 10.1007/s11655-019-3166-8. Epub ahead of print. PMID: 31227964.]

Comment 3 An acronym that appears in 'Figure legends' requires specification of its full name. And the authors need to make a detailed illustration of the staining grouping (PI, FITC and FITC-PI) of Fig. 4 to facilitate readers' understanding.

For Comment 3

We have defied all abbreviations in all figure legends.

Comment 4 Can FITC-dextran be used in an MI model? It is recommended to add an MI group to evaluate the use of FITC-dextrann for differentiating the MI model from the IR model. In addition, it is recommended to add staining that assesses MI (e.g. Masson) to assess the robustness of this IR model.

For Comment 4

Microvascular permeability is often used as a very important sign to evaluate severity of IR injury. However, in the majority of MI studies, endothelium cannot survive in infarction area because coronary arteries are ligatured permanently. So our method may be not that meaningful in MI model.

Anyway, we have test our method in MI model.

We injected 10%w/v FITC-dextran solution into rat's vein after ligation. After 3 hours, we sacrificed rats.
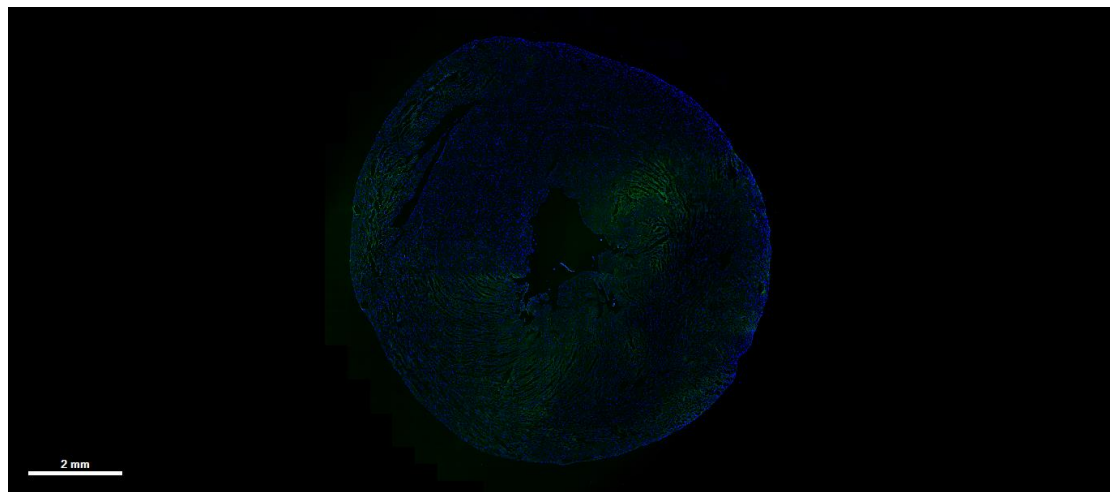
FITC-dextran cannot go through ligation site so there is little fluorescence in infarction area.

Next, we injected 10%w/v FITC-dextran solution into rat's vein 5 minutes before ligation. After 3 hours, we sacrificed rats and scan slides.
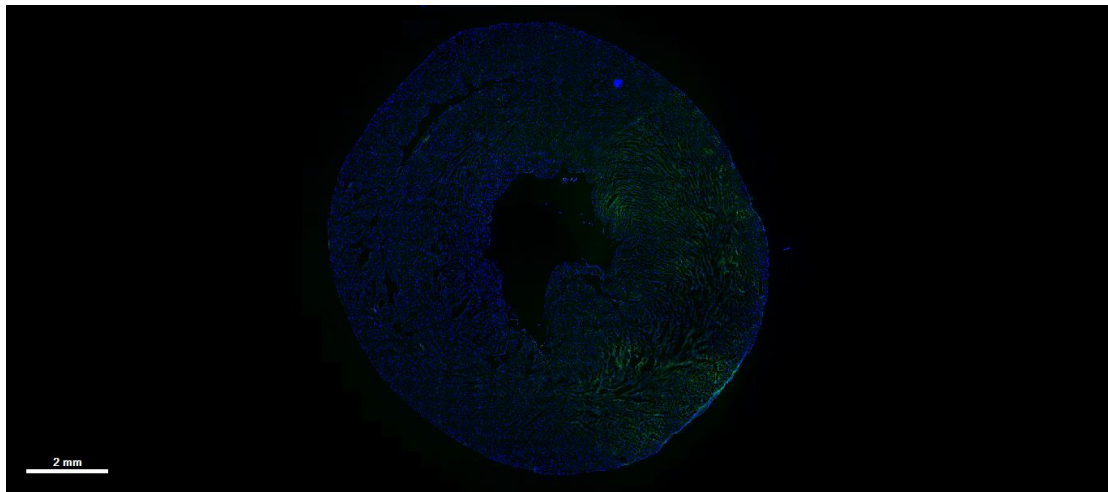
Unexpectedly, there is little fluorescence in infarction area. We estimate that it is almost no microcirculation in infarction area that cause this phenomenon.

Comment 5 Although the author explains the shortcomings of EB staining, it is only a hypothetical defect. Why not add an EB staining group and compare it with FITC-dextran group to get objective evidence?

For Comment 5

We have repeated our method with Evans blue. Evans blue can exactly be excited via Texas Red 594 channel and become a potential alternative. But, compared with FITC-dextran, EB shows inferior sensitivity and lower image quality. Detailed results have been display in our manuscript and supplemental materials.

Comment 6 The lack of electron microscopy results for endothelial cells is also an insufficiency of this study, although the mechanism by which FITC-dextran penetrates the endothelial barrier is elucidated in the 'Introduction'. There was no direct observation of endothelial cells in the results, which could not verify the damage of microvascular endothelial barrier of IR model.

For Comment 6

This protocol aims to evaluate microvascular permeability functionally but not to study endothelial microstructure. Previously, we have done electron microscopy to test endothelial injury induced by IR and protection of Tongxinluo.
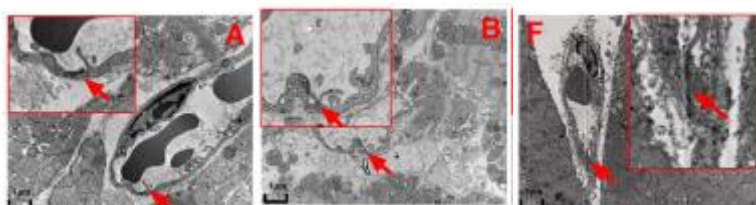
Sham animals showed a considerable overlap between adjacent endothelial cells

(ECs) (image A). Conversely, ECs from IR group appeared swollen with increased lysosomal-like inclusions and connection between ECs was destroyed (image B). After TXL treatment, ECs of hearts appeared elongated, attached with smooth contours, and connected well with adjacent ECs (image F).

[**Reference**: Qi K, Li X, Geng Y, Cui H, Jin C, Wang P, Li Y, Yang Y. Tongxinluo attenuates reperfusion injury in diabetic hearts by angiopoietin-like 4-mediated protection of endothelial barrier integrity via PPAR-α pathway. PLoS One. 2018 Jun 18;13(6): e0198403.]

ANSWERS TO Reviewer 2

We are also grateful for your suggestions and interest.

Comment 1 In this study, Tongxinluo capsule was selected as the treatment drug. What is the main reason for selection? Please give corresponding explanation in the introduction or discussion

For Comment 1

So far, there is few drug regarded recommended to cure myocardial ischemia-reperfusion injury in current clinical Guidelines. Many clinical and basic studies from our team suggest that Tongxinluo can indeed relieve microvascular collapse induce by IR, so we believe Tongxinluo can reverse injured endothelial barrier.

1. Our clinical trial suggests Tongxinluo could reduce myocardial no-reflow and infarction area significantly after emergency PCI for STEMI with conventional medicine therapy.

[**Reference**: No-reflow protection and long-term efficacy for acute myocardial infarction with Tongxinluo: a randomized double-blind placebo-controlled multicenter clinical trial (ENLEAT Trial)]. Another larger RCT of our team is in progress and its study design has been published.

[**Reference**: China Tongxinluo Study for myocardial protection in patients with Acute Myocardial Infarction (CTS-AMI): Rationale and design of a randomized, double-blind, placebo-controlled, multicenter clinical trial]

2. Our basic studies in swine and SD rat suggests Tongxinluio can alleviate infarct size after myocardial reperfusion and prevent endothelium from apoptosis.

Reference1:Tongxinluo reduces myocardial no-reflow and ischemia-reperfusion injury by stimulating the phosphorylation of eNOS via the PKA pathway.

Reference2:Cardiomyocyte-derived small extracellular vesicles can signal eNOS

activation in cardiac microvascular endothelial cells to protect against Ischemia/Reperfusion injury.

Reference3:Inhibition of miR-128-3p by Tongxinluo Protects Human Cardiomyocytes from Ischemia/reperfusion Injury via Upregulation of p70s6k1/p-p70s6k1.]

Comment 2 According to the fig1-fig2 experimental results, Tongxinluo has a good regulatory effect in improving the microvascular injury associated with I/R. what are its main active ingredients? please list

For Comment 2

Tongxinluo capsule was registered in the State Food and Drug Administration of China for treatment of angina pectoris in 1996. Tongxinluo (TXL), a special formula of Chinese traditional medicines, is composed of *Radix ginseng*, *Buthus martensi*, *Hirudo*, *Eupolyphaga seu steleophaga*, *Scolopendra subspinipes*, *Periostracum cicadae*, *Radix paeoniae rubra*, *Semen ziziphi spinosae*, *Lignum dalbergiae odoriferae*, *Lignum santali albi*, and *Borneolum syntheticum*.

Comment 3 If there are relevant preliminary Clinical or basic studies regarding to Tongxinluo? please list them.

For Comment 3

We have been studying tongxinluo protection to cardiac microvascular endothelial cell(CMEC) in MIRI model for over ten years. There have been 2 clinical trials designed (1,2)and dozens of basic researches conducted to explain effectiveness and mechanisms of tongxinluo (3-12).

1. Zhang HT, Yang YJ. No-reflow protection and long-term efficacy for acute myocardial infarction with Tongxinluo: a randomized double-blind placebo-controlled multicenter clinical trial (ENLEAT Trial). *Chin Med J (Engl).* 2010 Oct;123(20):2858-64. PMID: 21034597.

2. Xu Y,Peterson ED, Gao R, Yang Y. China Tongxinluo Study for myocardial protection in patients with Acute Myocardial Infarction (CTS-AMI): Rationale and design of a randomized, double-blind, placebo-controlled, multicenter clinical trial. *Am Heart J*. 2020 Sep;227:47-55. doi: 10.1016/j.ahj.2020.06.011. Epub 2020 Jun 20. PMID: 32679281; PMCID: PMC7305744.

3. Chen G, Xu C, Gillette TG, Hill JA, Yang Y. Cardiomyocyte-derived small extracellular vesicles can signal eNOS activation in cardiac microvascular endothelial cells to protect against Ischemia/Reperfusion injury. *Theranostics.* 2020 Sep 23;10(25):11754-11774. doi: 10.7150/thno.43163. PMID: 33052245; PMCID: PMC7546010.

4. Li Q, Li N, Yang YJ. Tongxinluo exerts protective effects via anti-apoptotic and pro-autophagic mechanisms by activating AMPK pathway in infarcted rat hearts. *Exp Physiol.* 2017 Apr 1;102(4):422-435. doi: 10.1113/EP086192. Epub 2017 Mar 14. PMID: 28150462.

5. Li XD, Yang YJ. Tongxinluo reduces myocardial no-reflow and ischemia-reperfusion injury by stimulating the phosphorylation of eNOS via the PKA pathway. *Am J Physiol Heart Circ Physiol.* 2010 Oct;299(4):H1255-61. doi: 10.1152/ajpheart.00459.2010. Epub 2010 Aug 6. PMID: 20693395.

6. Qi K, Yang Y. Tongxinluo attenuates oxygen-glucose-serum deprivation/restoration -induced endothelial barrier breakdown via peroxisome proliferator activated receptor-a/angiopoietin-like 4 pathway in high glucose-incubated human cardiac microvascular endothelial cells. *Medicine (Baltimore).* 2020 Aug 21;99(34):e21821. doi: 10.1097/MD.0000000000021821. PMID: 32846824; PMCID: PMC7447398.

7. Li Q, Cui HH, Yang YJ. Quantitative Proteomics Analysis of Ischemia/Reperfusion Injury-Modulated Proteins in Cardiac Microvascular Endothelial Cells and the Protective Role of Tongxinluo. *Cell Physiol Biochem.* 2017;41(4):1503-1518. doi: 10.1159/000470806. Epub 2017 Mar 24. PMID: 28334711.

8. Qi K, Yang Y. Tongxinluo attenuates reperfusion injury in diabetic hearts by angiopoietin-like 4-mediated protection of endothelial barrier integrity via PPAR-α pathway. *PLoS One.* 2018 Jun 18;13(6):e0198403. doi: 10.1371/journal.pone. 0198403. PMID: 29912977; PMCID: PMC6005559.

9. Cui H, Yang Y. Tongxinluo modulates cytokine secretion by cardiac microvascular endothelial cells in ischemia/reperfusion injury. *Am J Transl Res.* 2016 Oct 15;8(10): 4370-4381. PMID: 27830021; PMCID: PMC5095330.

10. Qi K, Yang Y. Cardiac microvascular barrier function mediates the protection of Tongxinluo against myocardial ischemia/reperfusion injury. *PLoS One.* 2015 Mar 17;10(3):e0119846. doi: 10.1371/journal.pone.0119846. PMID: 25781461; PMCID: PMC4363146.

11. Cui H, Yang Y. Induction of autophagy by Tongxinluo through the MEK/ERK pathway protects human cardiac microvascular endothelial cells from hypoxia/ reoxygenation injury. *J Cardiovasc Pharmacol.* 2014 Aug;64(2):180-90. doi: 10.1097/FJC.0000000000000104. PMID: 24705173.

12. Chen G, Yang Y, Xu C, Gao S. A Flow Cytometry-based Assay for Measuring Mitochondrial Membrane Potential in Cardiac Myocytes After Hypoxia/ Reoxygenation. *J Vis Exp.* 2018 Jul 13;(137):57725. doi: 10.3791/57725. PMID: 30059023; PMCID: PMC6126459.

Besides, Tongxinluo has also been studied in IR model of central nervous

system(1,2,3,4) and intestine(5,6).

1. Cai M, Cai D. Tongxinluo reduces brain edema and inhibits post-ischemic inflammation after middle cerebral artery occlusion in rats. *J Ethnopharmacol.* 2016 Apr 2;181:136-45. doi: 10.1016/j.jep.2016.01.026. Epub 2016 Jan 21. PMID: 26805468.

2. Yu Z, Cai D. Neuroprotective effects of Tongxinluo on focal cerebral ischemia and reperfusion injury in rats associated with the activation of the MEK1/2/ERK1/2/ p90RSK signaling pathway. *Brain Res.* 2018 Apr 15;1685:9-18. doi: 10.1016/j.brainres. 2018.01.036. Epub 2018 Feb 7. PMID: 29425910.

3. Cheng X, Cai Y. Protective effects of Tongxinluo on cerebral ischemia/reperfusion injury related to Connexin43/Calpain II/Bax/Caspase-3 pathway in rat. *J Ethnopharmacol.* 2017 Feb 23;198:148-157. doi: 10.1016/j.jep.2017.01.004. Epub 2017 Jan 5. PMID: 28065778.

4. Yu ZH, Cai DF. PI3K/Akt pathway contributes to neuroprotective effect of Tongxinluo against focal cerebral ischemia and reperfusion injury in rats. *J Ethnopharmacol.* 2016 Apr 2;181:8-19. doi: 10.1016/j.jep.2016.01.028. Epub 2016 Jan 22. PMID: 26805466.

5. Zhang JX, Li SD, Liu Y, Yang MH. Preventive effect of Tongxinluo on endothelial survival and vascular integrity, together with inhibition of inflammatory reaction in rats model of intestine ischemia/reperfusion injury. *Pak J Pharm Sci.* 2018 Nov;31(6):2403-2410. PMID: 30473511.

6. Junxiu Z, Shaodan L. Mast cell activation, TLR4-NF-κB/TNF-α pathway variation in rats' intestinal ischemia-reperfusion injury and Tongxinluo's therapeutic effect. *Pak J Pharm Sci.* 2020 Jul;33(4):1599-1608. PMID: 33583793.

Comment 4 Regarding to coronary microvascular injury in myocardial ischemia/reperfusion they are referred to (and should possibly cite):

1. Zhou H, Wang J, Zhu P, Zhu H, Toan S, Hu S, Ren J, Chen Y. NR4A1 aggravates the cardiac microvascular ischemia reperfusion injury through suppressing FUNDC1-mediated mitophagy and promoting Mff-required mitochondrial fission by CK2α. Basic Res Cardiol. 2018 May 9;113(4):23. doi: 10.1007/s00395-018-0682-1. PMID: 29744594.

2. Wang J, Toan S, Zhou H. Mitochondrial quality control in cardiac microvascular ischemia-reperfusion injury: New insights into the mechanisms and therapeutic potentials. Pharmacol Res. 2020 Jun;156:104771. doi: 10.1016/j.phrs.2020.104771. Epub 2020 Mar 28. PMID: 32234339.

3. Zhu H, Tan Y, Du W, Li Y, Toan S, Mui D, Tian F, Zhou H. Phosphoglycerate mutase

5 exacerbates cardiac ischemia-reperfusion injury through disrupting mitochondrial quality control. Redox Biol. 2021 Jan;38:101777. doi: 10.1016/j.redox.2020.101777. Epub 2020 Nov 1. PMID: 33166869; PMCID: PMC7658715.

4. Heusch G. The Coronary Circulation as a Target of Cardioprotection. Circ Res. 2016 May 13;118(10):1643-58. doi: 10.1161/CIRCRESAHA.116.308640. PMID: 27174955.

5.Heusch G, Gersh B. The pathophysiology of acute myocardial infarction and strategies of protection beyond reperfusion: a continual challenge. European heart journal. 2017; 38: 774-84.

For Comment 4

Currently, mitochondrial homeostasis is a highlight in the domain of cardioprotection in IR model. We have read them and cited first three of them in Discussion.

Comment 5 There are English mistakes appeared in the text. So, I recommend the authors to have conducted the English revision by English native editors.

For Comment 5

Thanks for your suggestion, we have refined our manuscript and correct our mistakes.

Comment 6 The resolution of the picture is too low. Please provide high definition figure, such as figure4-5.

For Comment 6

We have tried our best to modify our figure in our new manuscript. If editors do not satisfy images, we can provide original .tiff snapshots.

Comment 7 What is the main participation or regulation mechanism of VE-cadherin, β-catenin, JAM-A and Occludin in microvascular injury? If there are relevant studies, please list them.

For Comment 7

VE-cadherin is a key element of endothelial cell-to-cell adhesion junctions, and it contributes a lot to the maintenance of vascular integrity. Furthermore, β-catenin connects to VE-cadherin directly and structurally to maintain endothelial intercellular junctions.

VE-cadherin AND β-catenin
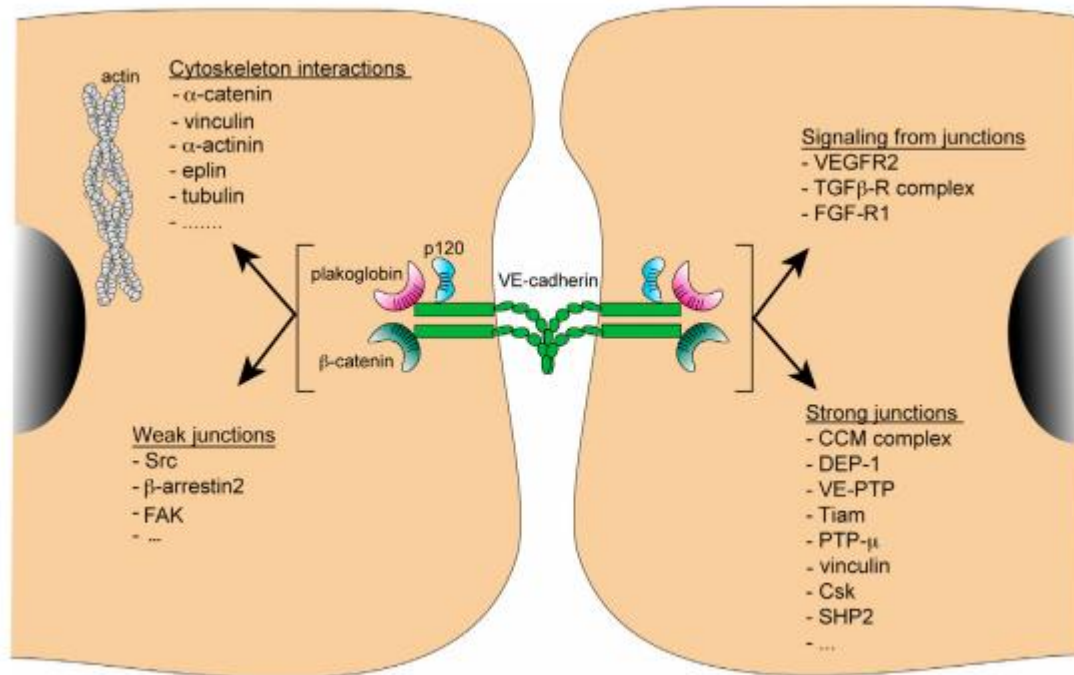
[This illustration was cited from "VE-cadherin and endothelial adherens junctions: active guardians of vascular integrity. Dev Cell. 2013 Sep 16;26(5):441-54. doi: 10.1016/j.devcel.2013.08.020. PMID: 24044891."]

Vestweber D. VE-cadherin: the major endothelial adhesion molecule controlling cellular junctions and blood vessel formation. *Arterioscler Thromb Vasc Biol.* 2008 Feb;28(2):223-32. doi: 10.1161/ATVBAHA.107.158014. Epub 2007 Dec 27. PMID: 18162609.

Giannotta M, Trani M, Dejana E. VE-cadherin and endothelial adherens junctions: active guardians of vascular integrity. *Dev Cell.* 2013 Sep 16;26(5):441-54. doi: 10.1016/j.devcel.2013.08.020. PMID: 24044891.

Lampugnani MG, Dejana E, Giampietro C. Vascular Endothelial (VE)-Cadherin, Endothelial Adherens Junctions, and Vascular Disease. *Cold Spring Harb Perspect Biol.* 2018 Oct 1;10(10):a029322. doi: 10.1101/cshperspect.a029322.

Xiong S, Hong Z, Malik AB. IL-1β suppression of VE-cadherin transcription underlies sepsis-induced inflammatory lung injury. *J Clin Invest.* 2020 Jul 1;130(7):3684-3698. doi: 10.1172/JCI136908. PMID: 32298238; PMCID: PMC7324198.

Broman MT, Kouklis P, Malik AB. Cdc42 regulates adherens junction stability and endothelial permeability by inducing alpha-catenin interaction with the vascular endothelial cadherin complex. *Circ Res.* 2006 Jan 6;98(1):73-80. doi: 10.1161/01. RES.0000198387.44395.e9. Epub 2005 Dec 1. PMID: 16322481

Occludin AND JAM-A

Feldman GJ, Mullin JM, Ryan MP. Occludin: structure, function and regulation. *Adv Drug Deliv Rev.* 2005 Apr 25;57(6):883-917. doi: 10.1016/j.addr.2005.01.009. PMID: 15820558.

Fang M, Zhong WH, Wang HD. Ulinastatin Ameliorates Pulmonary Capillary Endothelial Permeability Induced by Sepsis Through Protection of Tight Junctions via Inhibition of TNF-α and Related Pathways. *Front Pharmacol.* 2018 Aug 13;9:823. doi: 10.3389/fphar.2018.00823. PMID: 30150933; PMCID: PMC6099086.

Kakogiannos N, Ferrari L, Giannotta M. JAM-A Acts via C/EBP-α to Promote Claudin-5 Expression and Enhance Endothelial Barrier Function. *Circ Res.* 2020 Sep 25;127(8):1056-1073. doi: 10.1161/CIRCRESAHA.120.316742. Epub 2020 Jul 15. PMID: 32673519; PMCID: PMC7508279.

Tang L, Zhang C, Zhang J. Melatonin maintains inner blood-retinal barrier via inhibition of p38/TXNIP/NF-κB pathway in diabetic retinopathy. *J Cell Physiol.* 2021 Aug;236(8):5848-5864. doi: 10.1002/jcp.30269. Epub 2021 Jan 11. PMID: 33432588.

Zhang Y, Li X,Liu W. Occludin degradation makes brain microvascular endothelial cells more vulnerable to reperfusion injury in vitro. *J Neurochem*. 2021 Feb;156(3):352-366. doi: 10.1111/jnc.15102. Epub 2020 Jul 7. PMID: 32531803.

In summary, we mainly tested Evans blue in our method and found that EB may be a sub-optimal alternative. Besides, the majority of drawbacks have been corrected in our renewed manuscript. Our team are very grateful for all kind comments and suggestions from editors and reviewers.

Yours sincerely

Yuejin Yang

yangyjfw@126.com

June 2, 2021